Electronic Supplementary Material (ESI) for Journal of Materials Chemistry B.

Supplementary document

A Muscle Mimetic Polyelectrolyte-Nanoclay Organic-Inorganic Hybrid Hydrogel: Its Self-healing, Shape-memory and Actuation Properties

Sovan Lal Banerjee[a], Thomas Swift[b], Richard Hoskins,[b] Stephen Rimmer[b]*, Nikhil K. Singha[a]*

[a]Rubber Technology Centre, Indian Institute of Technology, Kharagpur, India.

[b]School of Chemistry and Biosciences, University of Bradford, Bradford, West Yorkshire BD7 1DP, U.K.

*Email - nks@rtc.iitkgp.ernet.in, nks8888@yahoo.com

FTIR and XRD Analysis

Figure S1(a) shows the FTIR spectra of soluble starch, starch-*g*-PMTAC, pure hydrogel and composite hydrogel. The spectrum for starch, contained a broad peak near 3416 cm^{-1} was attributed to the existence of –OH stretching. The absorption band for $–CH_2$ stretching vibration was observed near 2927 cm^{-1}. A vibration band near 1163 cm^{-1} was due to the presence of C-O-C bond. In the case of the as-prepared hydrogel ($PSAS_{50}C_0$), the vibration peaks at 1394 cm^{-1}, and 1731 cm^{-1} were due to the presence of in-plane deformations of –CH bond and >C=O stretching. The absorption bands at 1491 cm^{-1} and 942 cm^{-1} were due to the bending and stretching vibration of the quaternary ammonium group respectively. The existence of the peak near 1560 cm^{-1} signifies the presence of $–COO^-$ of poly(sodium acrylate). This indicated the probability of the formation of the ionic bond between $–COO^-$ and $–N(CH_3)_3^+$ through electrostatic interactions[1]. In the case of the composite hydrogel, characteristic transmittance peaks for CTAB modified MMT appeared at 3630 cm^{-1} and 3395 cm^{-1} (presence of free –OH and bound –OH of OMMT), 1478 cm^{-1} ($–CH_3$ bending vibration of the quaternary ammonium ion $[RN(CH_3)_3]^+$of CTAB) respectively.

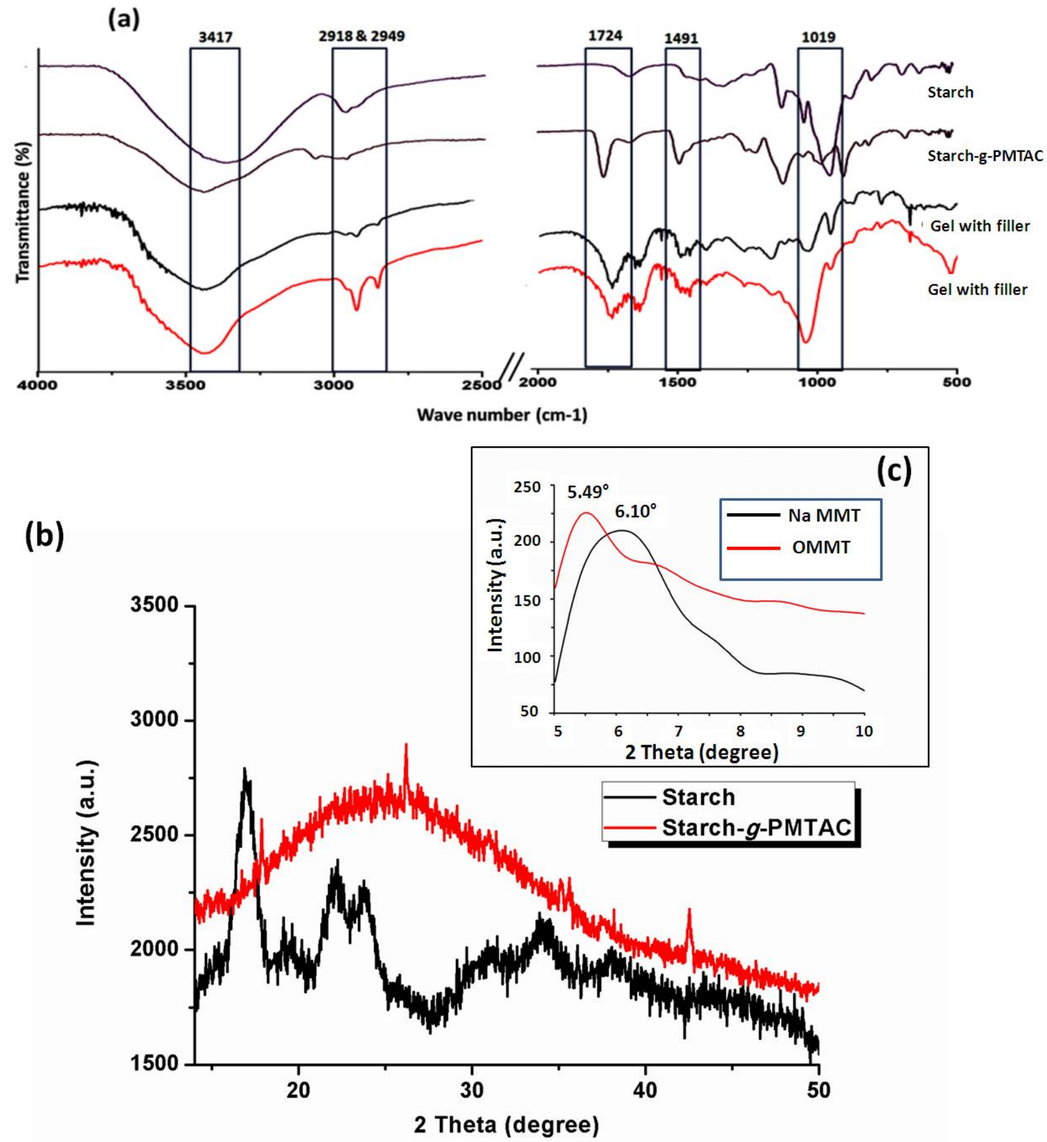

Figure S1. (a) FTIR analysis, (b) & (c) XRD analysis.

Determination of the hydrodynamic radii from the DOSY NMR analysis

Equation S1: Equations used to determine hydrodynamic radii of polymers:

$$D = \frac{k_B T}{6\pi\eta r}$$

$$R_H = \frac{k_B T}{6\pi\eta D}$$

$$D_1\eta_1 = D_2\eta_2$$

Where, D = Diffusion coefficient; T = absolute temperature; η = viscosity of the solvent; R_H = hydrodynamic radius; k_B = Boltzmann constant.

Diffusion of D_2O at 298 K = 1.93 x10^{-9} m^2 S^{-1}.

Diffusion of Soluble Starch at 298 K = 1.99 x10^{-11} m^2 S^{-1}.

Diffusion of D_2O (solvent) with Soluble Starch at 298 K = 2.04 x10^{-9} m^2 S^{-1}.

Diffusion of Starch-PMTAC at 298 K = 4.89 x10^{-12} m^2 S^{-1}.

Diffusion of D_2O (solvent) with Starch-PMTAC at 298 K = 1.86 x10^{-9} m^2 S^{-1}.

R_{Hp} soluble starch at 298 K = 10.6 nm

R_{Hp} Starch-PMTAC at 298 K = 39.2 nm

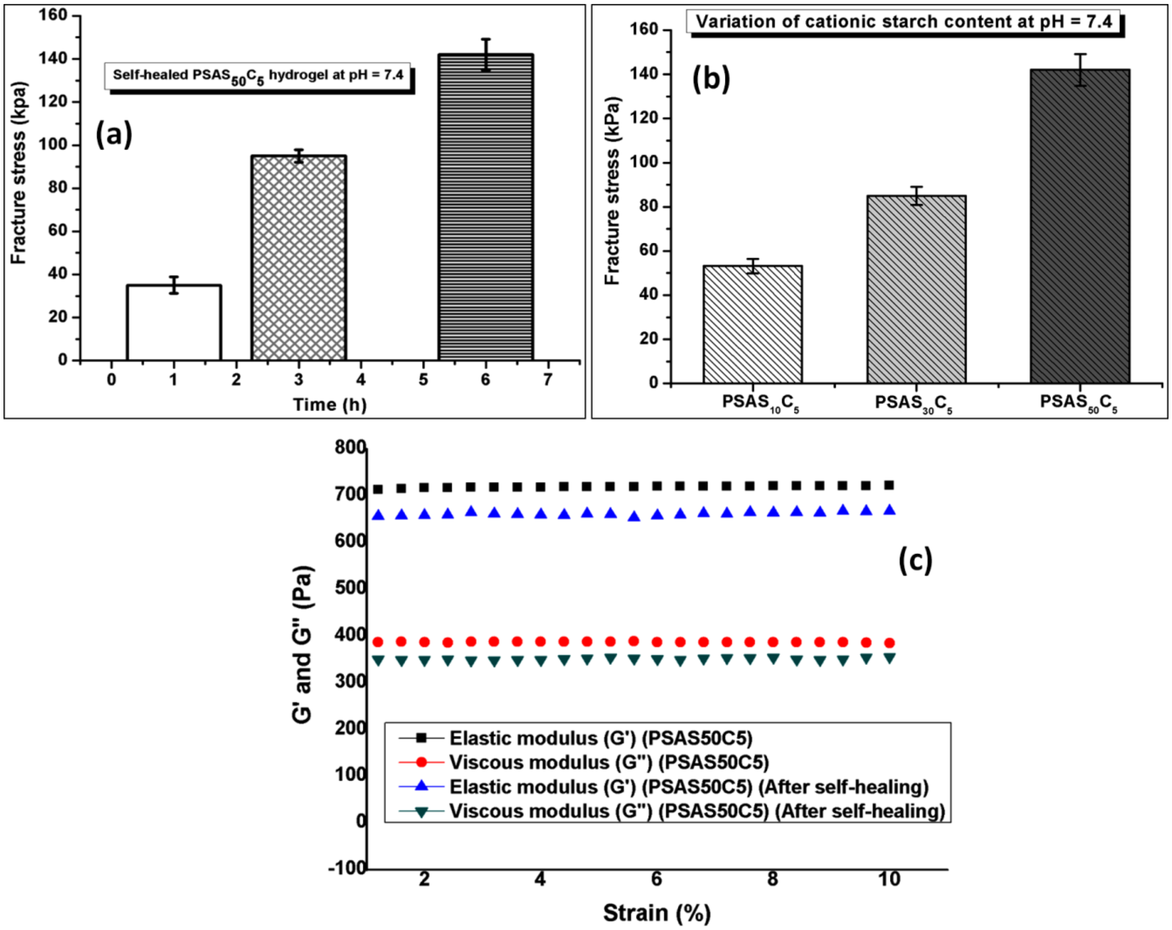

Figure S2: (a) & (b) Comparison of the fracture stress with the variation in the self-healing time and content of cationic starch respectively; **(c)** self-healing study through rheological analysis.

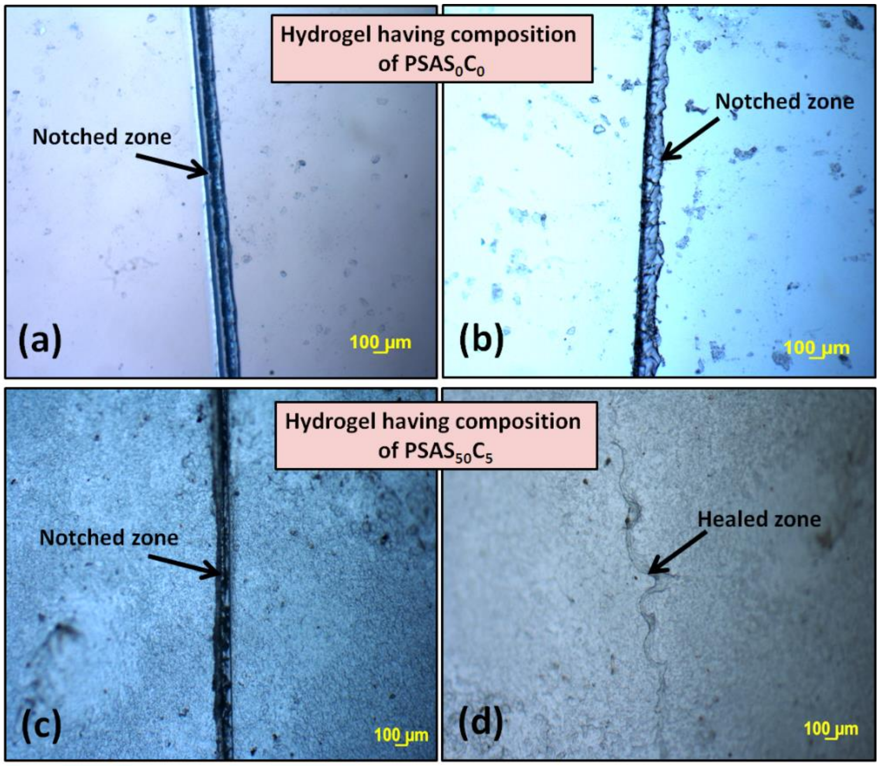

Figure S3: Self-healing study of the hydrogel via 'scratch & heal" method analysed through optical microscopy- **(a)** & **(b)** anionic hydrogel ($PSAS_0C_0$) before and after buffer (pH 7.4) treatment; **(c)** & **(d)** composite hydrogel ($PSAS_{50}C_5$) before and after buffer (pH 7.4) treatment.

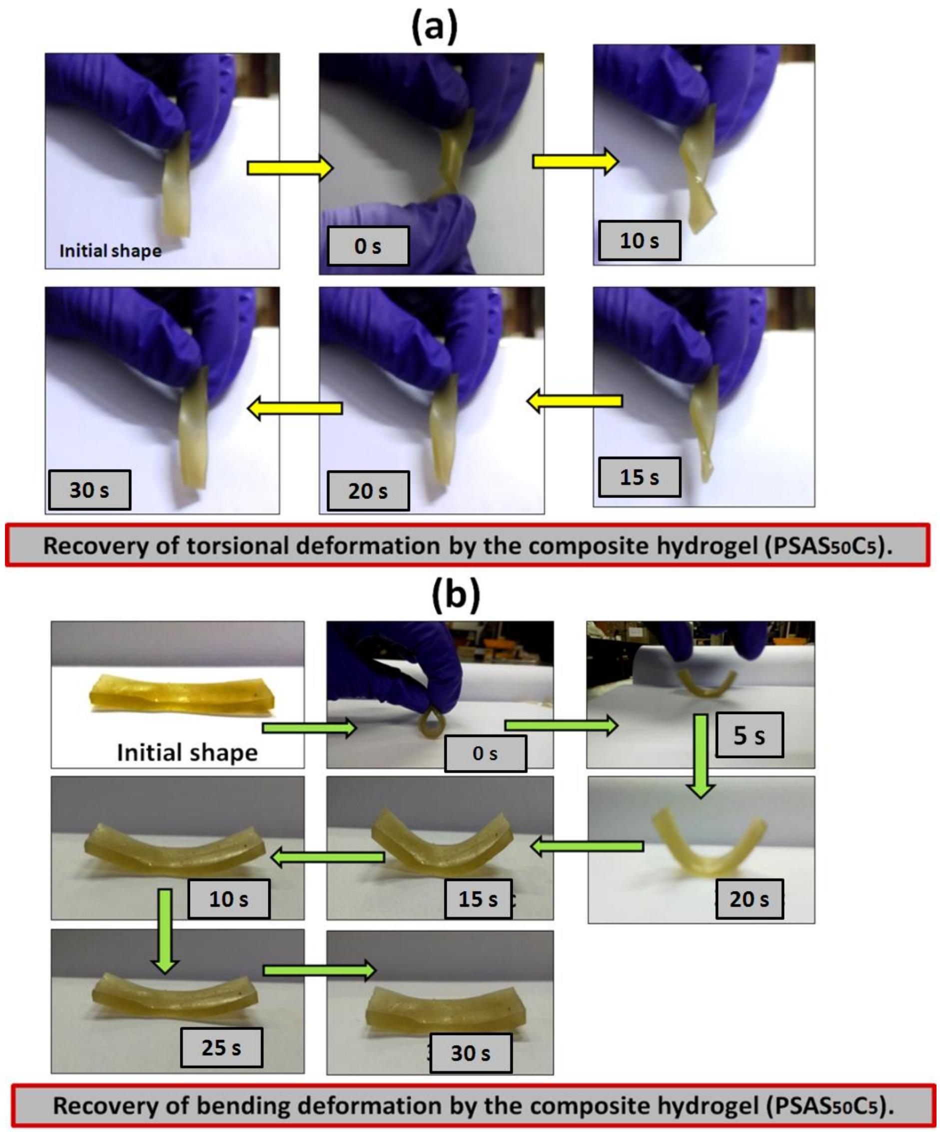

Figure S4: Shape recovery study after the application of **(a)** torsional force and **(b)** bending force.

Table S1: Repeatability study of the water based shape memory effect

No of cycle	Shape fixity (R_f) (%)	Shape recovery (R_r) (%)
1	**>95**	**90**
2	**>95**	**90**
3	**>93**	**88**

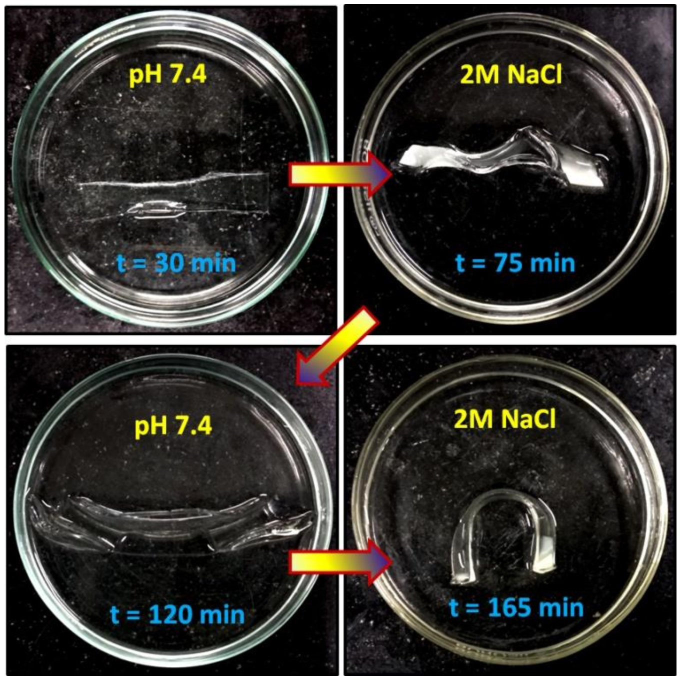

Figure S5: Salt induced actuation in the control hydrogel system ($PSAS_0C_0$) (anionic hydrogel) having no cationic segment.

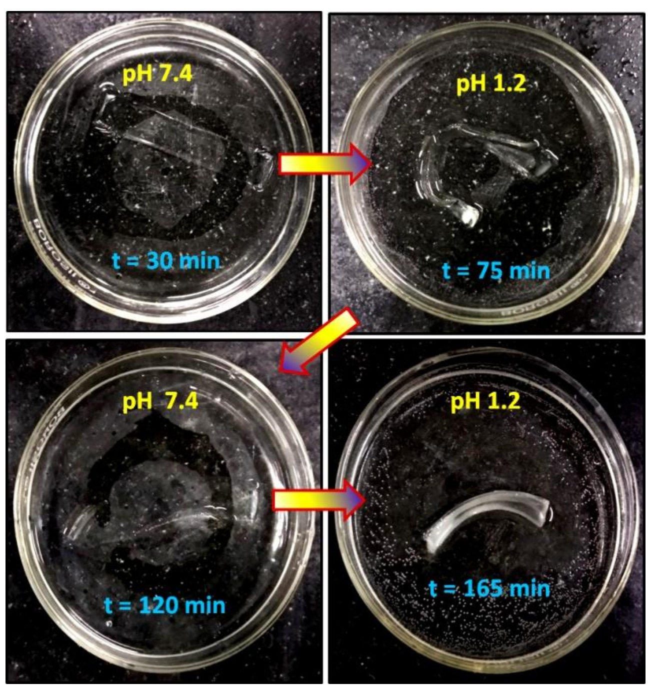

Figure S6: Acid induced actuation in the control hydrogel system ($PSAS_0C_0$) (anionic hydrogel) having no cationic segment.

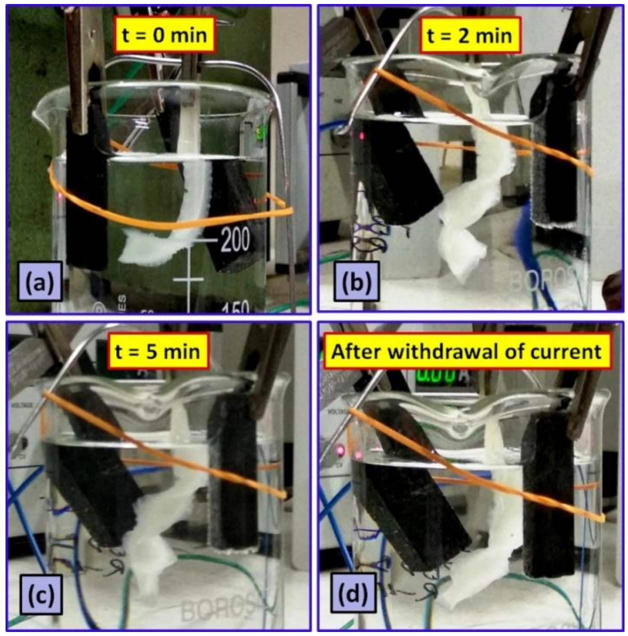

Figure S7: Image of the custom built voltameter and orientation of the polyelectrolyte hydrogel strip at **(a)** t = 0 min, **(b)** 2 min, **(c)** 5 min of current flow and **(d)** after the withdrawal of the current.

71

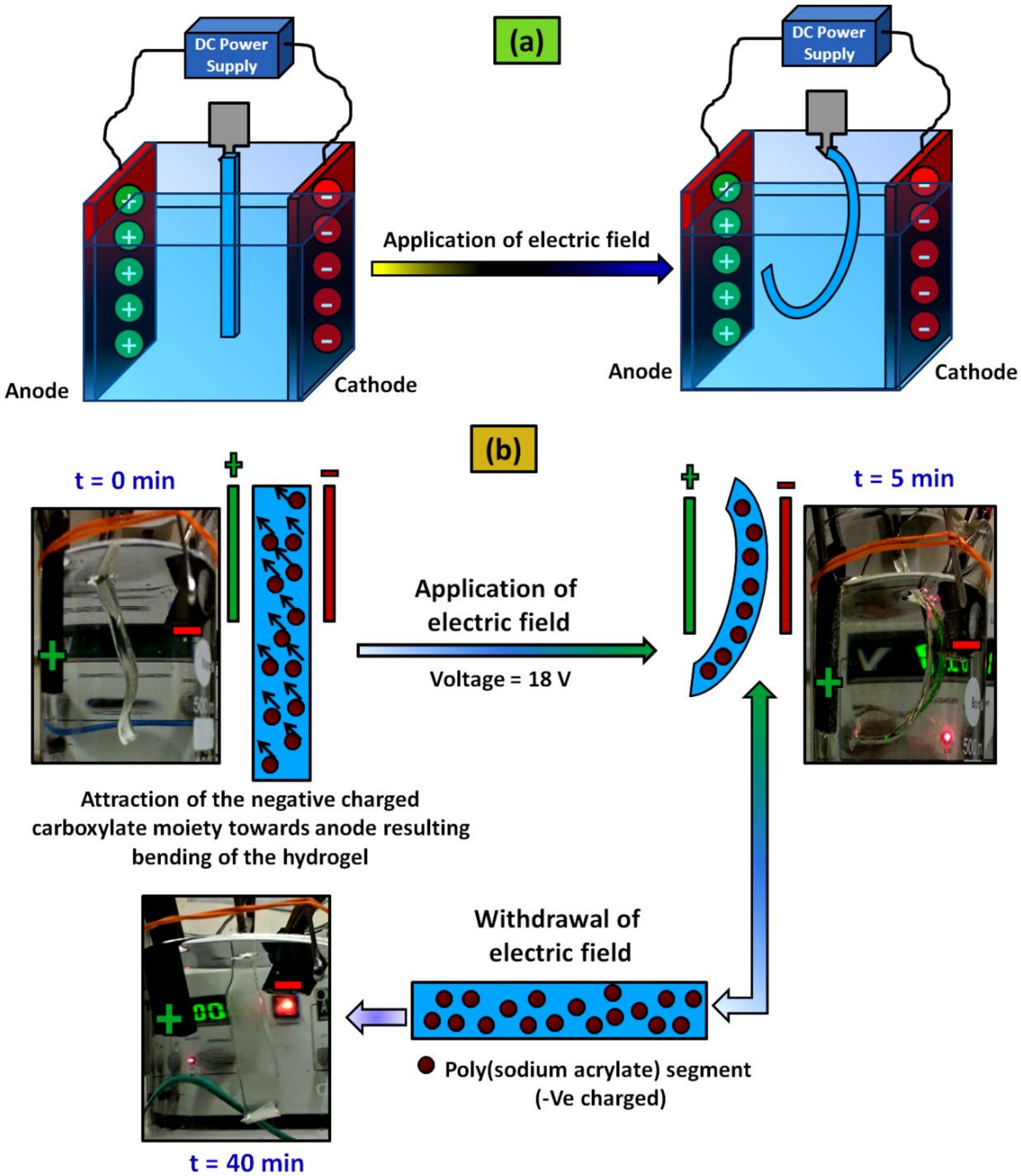

72 **Figure S8: (a)** Schematic representation of the actuation in the polyelectrolyte anionic hydrogel
73 ($PSAS_0C_0$) system in the presence of an electrical field and **(b)** behaviour of the anionic hydrogel
74 ($PSAS_0C_0$) system with the time of electric field application.

75 **References**

76 1. Y. Huang, J. Lu and C. Xiao, Polymer degradation and stability, 2007, **92**, 1072-1081.

77